Published in final edited form as:
J Nat Prod. 2010 June 25; 73(6): 1188–1191. doi:10.1021/np100203x.

Xestosaprols from the Indonesian Marine Sponge *Xestospongia* sp.

Jingqiu Dai[†], **Analia Sorribas**[†], **Wesley Y. Yoshida**[†], **Michelle Kelly**[‡], and **Philip G. Williams**[†,⊥,*]

Department of Chemistry, University of Hawaii at Manoa, Honolulu, Hawaii, 96822, The Cancer Research Center of Hawaii, 651 Ilalo Street, Honolulu, Hawaii, 96813, National Centre for Aquatic Biodiversity and Biosecurity, National Institute of Water & Atmospheric Research, Ltd, 41 Market Place, Auckland Central 1010, New Zealand.

[†] University of Hawaii

[‡] National Institute of Water & Atmospheric Research

[⊥] Cancer Research Center of Hawaii

Eight pentacyclic compounds, xestosaprols F-M (**1-8**), were isolated from a marine sponge belonging to the genus *Xestospongia*. The structures of these new compounds were determined on the basis of extensive analyses of NMR experiments and mass spectrometric measurements. These compounds inhibited the aspartic protease, BACE1, at moderate levels in a dose-dependent manner.

Marine organisms are rich sources of structurally-diverse compounds.[1,2,3] These unique secondary metabolites exhibit a diverse array of biological activities ranging from antimicrobial to anticancer.[4,5,6] As part of a systematic evaluation of marine invertebrates for new drug leads for neurological disorders, we recently published the isolation of xestosaprols D and E from a species of *Xestospongia* (Order Haplosclerida: Family Petrosiidae) from Indonesia.[7] To further our understanding of the factors responsible for their biological activity, we examined several other extracts derived from *Xestospongia* spp. collected in the same Indo-Pacific location for congeners of this structural class. Work with one such extract has now led to the isolation and structure elucidation of eight related compounds, which are reported here, along with their biological activity against BACE1.

A sample of the sponge *Xestospongia* sp., collected from Indonesia, was exhaustively extracted with MeOH. The pooled extracts were subjected to a modified Kupchan partitioning scheme to yield hexane, EtOAc, and *n*-butanol fractions as detailed in the Experimental Section. The EtOAc-soluble material was separated by repeated reversed-phase HPLC to afford xestosaprols F-M (**1-8**).

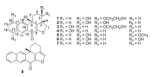

Compound **1**, which was obtained as a yellow solid, displayed a prominent pseudomolecular ion at *m/z* 367.1540 $[M + H]^+$ in the HRMS data indicating a molecular formula of $C_{22}H_{22}O_5$ and 12 double bond equivalents. The IR spectrum of xestosaprol F (**1**) showed

*To whom correspondence should be addressed: Tel. 808-956-5720. Fax: 808-956-5908. philipwi@hawaii.edu..

Supporting Information Available: Copies of the ^1H, ^{13}C, and 2D NMR spectroscopic data for all new compounds associated with this article and a photo of the producing organism are available free of charge via the Internet at http://pubs.acs.org.

strong absorptions for hydroxy (3382 cm^{-1}) and α,β-unsaturated ketone moieties (1649 cm^{-1}). The presence of this latter functional group was also supported by the resonance observed at 178.4 ppm in the ^{13}C NMR spectrum. Further analyses of the ^{13}C (Table 2) and multiplicity-edited HSQC NMR spectra showed the 22 carbon resonances could be ascribed to five methylenes, seven methines, and nine quaternary carbons, in addition to a single methyl group. On the basis of chemical shift considerations, 12 of these carbons, in addition to the carbonyl resonance, were sp^2 hybridized indicating **1** contained six carbon-carbon double bonds and five rings. The aromaticity of some of these rings was evident by the characteristic downfield shifts observed for five methine resonances in the ^1H NMR spectrum (δ_H 9.21, 8.07, 7.51, 7.50, and 6.94).

The planar structure of **1** was assembled through interpretation of the 2D NMR data (Figure 1). Analysis of the COSY spectrum of **1** established three discrete spin systems. The first system (**A**) was an ethylene glycol subunit comprised of H_2-21 and H_2-22. The second fragment (**B**) consisted of a linear chain of all the remaining sp^3 hybridized methines and methylenes that were identified in the spectroscopic data (H_2-1, H-2, H-3, H_2-4, H_2-5), with C-1 and C-3 deshielded by oxygens on the basis of their low field chemical shift ($\delta_{C\text{-}1}$ 72.5 and $\delta_{C\text{-}3}$ 68.6). The final system (**C**) that was deduced directly from analyses of the COSY spectrum consisted of three aromatic protons H-14, H-15, and H-16, in succession. HMBC correlations from the aromatic protons H-11 (δ_H 9.21) and H-18 (δ_H 8.07), which were singlets, established a central benzene ring consisting of carbons-10,-11,-12,-17,-18, and -19 to which all other residues in the molecule were related. The subsystem **C** was appended to this ring on the basis of 3-bond HMBC correlations from H-18 to C-16 and H-14 to C-12, but required that the oxygenated sp^2 carbon ($\delta_{C\text{-}13}$ 157.3) was placed in between the latter pair, based on HMBC correlations from H-11 and H-14. A HMBC correlation from H_2-21 to C-13 established the ethylene glycol fragment (**A**) was attached via an ether linkage to C-13. This larger system was then connected to fragment **B** based on HMBC correlations from the sole methyl singlet H_3-20, which in conjunction with correlations observed from H_2-1 and H-2 established the pentacyclic planar structure depicted.

The relative configuration of **1** was established by analysis of the magnitudes of the proton-proton couplings observed to the stereogenic centers and ROESY experiments. ROESY cross-peaks between H-2/H_3-20, H-2/H-4*β* (δ_H 1.92) and H-20/4*β* established the β-orientation of these protons. As the magnitude of the coupling constants observed within this ring were consistent with a chair conformer, the series of small couplings evident for H-3 established an equatorial position on the β-face of the molecule. These observations are consistent with the broad singlet observed for the equatorial proton at C-3 in the previously reported xestosaprol A as well.[3]

Compound **2** was obtained as a yellow powder. Comparison of the NMR spectra of **2** (Tables 1 and 2) with those of **1** revealed that **2** possessed a similar structure, except for the absence of the resonances corresponding to the ethylene glycol residue observed in **1**. Analysis of the HRMS data for **2** yielded a molecular formula of $C_{20}H_{18}O_4$ that was C_2H_4O smaller than that observed for **1**. Analysis of the ^{13}C NMR and DEPT spectra confirmed the loss of this unit and the formation of the corresponding phenolic compound. Therefore, **2** was assigned the trivial name xestosaprol G.

Xestosaprol H (**3**) was clearly an isomer of **1** based on the identical molecular formula ($C_{22}H_{22}O_5$) obtained by HRESIMS. Comparison of the ^1H, ^{13}C and 2D NMR spectra of **3** (Tables 1 and 2) with those of **1** revealed a notable upfield shift for H-3 (**1** $\delta_{H\text{-}3}$ 4.06; **2** $\delta_{H\text{-}3}$ 3.51) consistent with a configurational change that removed this proton from the deshielding effect of the σ electrons of the β-carbon-carbon bond. This conclusion was confirmed by a NOE correlation between H-3 and H-5α and the two large three bond proton-proton

couplings displayed by H-3 (Figure 2). These data established that **3** was epimeric to **1** at this position.

The structures of the remaining compounds were determined, in a similar fashion, to differ principally in the configuration at C-3 and the degree/location of oxidation. For example, xestosaprol I (**4**) was 13-deoxy-3-*epi*-xestosaprol G. Xestosaprol J (**5**) and K (**6**) were analogs of **2** that were hydroxylated at C-16 rather than C-13. The former compound was the methyl ether, while the latter possessed a free hydroxy group. Compound **7**, xestosaprol L, was the C-3 epimer of **4**. A molecular formula of $C_{20}H_{16}O_2$ was deduced from the HRMS and ^{13}C NMR data of xestosaprol M (**8**). These data established that **8** contained two additional sp^2 carbons which were attributed to oxidation of the dihydrofuran ring to the corresponding furan (Figure 3).

In biological screening, xestosaprols F-M showed moderate inhibition of the aspartic protease (Table 4), BACE1 (memapsin-2), which has a central role in the etiology of Alzheimer's disease. Compound **3** displayed the lowest IC_{50} value at 81 μM. Based on these data, it appears that a beta-orientation of the C-3 alcohol is required for activity as the corresponding epimer **1** is significantly less active.

The ring core found in **1-8** was first identified by Scheuer and coworkers in halenaquinone.[4] Several analogs have been subsequently reported that differ primarily in the degree of oxidation in the A[8] and E-rings,[1] sulfonation[9] or the addition of another heterocycle.[1] There are two notable distinctions within this series of new compounds. In all other members of this chemical family the A-ring is substituted with two oxygens at C-16 and C-13. As such, compounds **1-7** are the first examples of a mono-oxygenated A-ring, while **8** is the only example of a dideoxy ring. Second, while derivatives with methylation or acylation of the oxygens in the E-ring have been reported,[3] ethylene glycol derivatives such as **1** and **3** have not been observed previously in this series. In fact, derivatization with this particular two-carbon subunit is rarely encountered in Nature. To the best of our knowledge, pyrotechnoic acid[10] is the only natural product containing a glycol ether. In this particular, case, the linkage is to a sp^3 rather than a sp^2 carbon as found in **1** and **3**.

Experimental Section

General Experimental Procedures

Optical rotations were measured on a Jasco-DIP-700 polarimeter at the sodium line (589 nm). UV spectra were obtained on a Hewlett-Packard 8453 spectrophotometer and IR spectra were measured as a thin film on a CaF_2 disc using a Perkin Elmer 1600 series FTIR. NMR spectra were acquired on a Varian Inova 500 MHz spectrometer operating at 500 (^1H) or 125 (^{13}C) MHz using the residual solvent signals as an internal reference (CD_3OD δ_H 3.30 ppm, δ_C 49.0 ppm). Samples were in 3 mm Shigemi tubes during NMR analyses. High-resolution mass spectrometry data were obtained on an Agilent LC-MSTOF with ES ionization in the positive mode. Gradient separations used a Shimadzu system consisting of LC-20AT Solvent Delivery Modules, a SPD-M20A VP Diode Photodiode Array Detector, and a SCL-20A VP System Controller. TLC analyses were performed on $Si_{60}F_{254}$ plates and visualized under UV or by heating after spraying with a 1% anisaldehyde solution in acetic acid/H_2SO_4 (50:1). Samples were weighted on a Mettler Toledo analytical balance.

Biological Material

The sponge was collected from a coral reef habitat at a depth of approximately 20 m from the sea bed surface, at Sangalaki, Indonesia (2° 04’ 59” N, 118° 23’ 41” E) on the 17th of March 1996. The sponge forms thick regular mounds and branches, and has a relatively smooth surface. The mounds and branches are tough but have a crumbly texture. The

external and internal coloration in life is dark reddish brown. The skeleton is composed of robust rounded meshes formed by thick tracts of robust oxeas 220-260 μm long. The sponge is a species of *Xestospongia* (Order Haplosclerida: Family Petrosiidae), that has been referred to previously as *X. subtriangularis* (Duchassaing et Michelotti, 1864) by Desqueyroux-Faundez (1987) for New Caledonian specimens. The species name is currently considered to be invalid and restricted to sponges in the western central Atlantic, from where the species was first described. Voucher specimens have been deposited in the Natural History Museum, London (BMNH 2009.8.12.1-2).

Extraction and Isolation

The freeze-dried sponge (93 g) was chopped into small pieces and then exhaustively extracted with MeOH (5 × 1 L) at room temperature to afford 6.0 g of lipophilic extract. The residue was suspended in H_2O and partitioned with hexane, EtOAc and *n*-BuOH. The EtOAc extract (2.0 g) was subjected to Si flash column chromatography eluting with a gradient of MeOH in CH_2Cl_2 to afford 12 fractions. The residue from fraction 6 (20 mg) was further purified by RP-HPLC (Luna C_8, 250 × 10 mm, a linear gradient from 30-90% MeOH in H_2O over 40 min, flow rate 3 mL/min, PDA and ELSD detection) to afford xestosaprol M (**8**, t_R 40.0 min, 0.3 mg, 0.0003% yield). Fraction 7 (50.0 mg) was separated by RP-HPLC (Luna C_8, 250 × 10 mm, a linear gradient from 10-30% MeCN in H_2O over 40 min then 30% MeCN in H_2O for an additional 30 min, flow rate 3 mL/min, PDA and ELSD detection) to yield xestosaprol K (**6**, t_R 45.0 min, 0.9 mg, 0.001% yield) and xestosaprol J (**5**, t_R 49.0 min, 0.7 mg, 0.0008% yield). Separation of fraction 9 (35 mg) by RP-HPLC (Luna C_8, 250 × 10 mm, a linear gradient from 10-30% MeCN in H_2O over 40 min, flow rate 3 mL/min, PDA and ELSD detection) afforded xestosaprol H (**3**, t_R 51.0 min, 0.3 mg, 0.0003% yield), xestosaprol F (**1**, t_R 53.0 min, 0.9 mg, 0.001% yield) and xestosaprol G (**2**, t_R 52.5 min, 0.5 mg, 0.0005% yield). Fraction 11 (20 mg) was separated by RP-HPLC (Luna C_8, 250 × 10 mm, a linear gradient from 10-30% MeCN in H_2O over 40 min and then 30% MeCN in H_2O over 30 min, flow rate 3 mL/min, PDA and ELSD detection) to yield xestosaprol L (**7**, t_R 40.0 min, 0.2 mg, 0.0002% yield) and xestosaprol I (**4**, t_R 41.0 min, 0.1 mg, 0.0001% yield).

Xestosaprol F (1): yellow powder; $[\alpha]_D^{22}$ +14 (*c* 0.2, MeOH); UV (MeOH) λ_{max} (log ε) 221 (4.2), 249 (3.8), 271 (3.8), 332 (3.4), 379 (3.4) nm; IR (CaF_2) ν_{max} 3382, 1649, 1619 cm^{-1}; See Tables 1 and 2 for NMR spectroscopic data; HRESI-TOFMS *m/z* 367.1540 $[M + H]^+$ (calcd for $C_{22}H_{23}O_5^+$, 367.1546; Δ = -1.5 ppm).

Xestosaprol G (2): yellow powder; $[\alpha]_D^{22}$ -8.7 (*c* 0.2, MeOH); UV (MeOH) λ_{max} (log ε) 224 (3.5), 271 (3.3), 335 (3.2), 364 (3.3) nm; IR (CaF_2) ν_{max} 3396, 1650, 1316 cm^{-1}; See Tables 1 and 2 for NMR spectroscopic data; HRESI-TOFMS *m/z* 323.1279 $[M + H]^+$ (calcd for $C_{20}H_{19}O_4^+$, 323.1283; Δ = -1.4 ppm).

Xestosaprol H (3): yellow powder; $[\alpha]_D^{22}$ -10 (*c* 0.2, MeOH); UV (MeOH) λ_{max} (log ε) 223 (3.7), 246 (3.4), 269 (3.4), 330 (3.0), 382 (2.8) nm; IR (CaF_2) ν_{max} 3417, 1650 cm^{-1}; See Tables 1 and 2 for NMR spectroscopic data; HRESI-TOFMS *m/z* 367.1540 $[M + H]^+$ (calcd for $C_{22}H_{23}O_5^+$, 367.1546; Δ = -1.5 ppm).

Xestosaprol I (4): yellow powder; $[\alpha]_D^{22}$ -27 (*c* 0.2, MeOH); UV (MeOH) λ_{max} (log ε) 217 (3.9), 242 (3.7), 264 (3.6), 325 (3.3) nm; IR (CaF_2) ν_{max} 3411, 1655 cm^{-1}; See Table 1 for NMR spectroscopic data; HRESI-TOFMS *m/z* 307.1326 $[M + H]^+$ (calcd for $C_{20}H_{19}O_3^+$, 307.1334; Δ = -2.7 ppm).

Xestosaprol J (5): yellow powder; $[\alpha]_D^{22}$ -42 (*c* 0.2, MeOH); UV (MeOH) λ_{max} (log ε) 220 (4.0), 270 (3.7), 332 (3.3) nm; IR (CaF_2) ν_{max} 3417, 1650 cm^{-1}; See Tables 1 and 2 for

NMR spectroscopic data; HRESI-TOFMS *m/z* 337.1434 $[M + H]^+$ (calcd for $C_{21}H_{21}O_4^+$, 337.1440; Δ = -1.7 ppm).

Xestosaprol K (6): yellow powder; $[\alpha]_D^{22}$ -20 (*c* 0.2, MeOH); UV (MeOH) λ_{max} (log ε) 222 (3.4), 273 (3.1), 335 (2.7) nm; IR (CaF_2) ν_{max} 3365, 1652, 1106 cm^{-1}; See Tables 1 and 2 for NMR spectroscopic data; HRESI-TOFMS *m/z* 323.1278 $[M + H]^+$ (calcd for $C_{20}H_{19}O_4^+$, 323.1283; Δ = -1.7 ppm).

Xestosaprol L (7): yellow powder; $[\alpha]_D^{22}$ -8.7 (*c* 0.2, MeOH); UV (MeOH) λ_{max} (log ε) 218 (3.9), 246 (3.7), 263 (3.6), 327 (3.4) nm; IR (CaF_2) ν_{max} 3420, 1651, 1319 cm^{-1}; See Tables 1 and 2 for NMR spectroscopic data; HRESI-TOFMS *m/z* 307.1329 $[M + H]^+$ (calcd for $C_{20}H_{19}O_3^+$, 307.1334; Δ = -1.7 ppm).

Xestosaprol M (8): yellow powder; $[\alpha]_D^{22}$ +17 (*c* 0.2, MeOH); UV (MeOH) λ_{max} (log ε) 221 (3.9), 259 (3.6), 324 (3.5), 364 (3.3) nm; IR (CaF_2) ν_{max} 3417, 2922, 2360, 1666, 1595 cm^{-1}; See Tables 1 and 2 for NMR spectroscopic data; HRESI-TOFMS *m/z* 289.1223 $[M + H]^+$ (calcd for $C_{20}H_{17}O_2^+$, 289.1229; Δ = -1.9 ppm).

BACE1 Assay: β-Secretase mediated cleavage of amyloid precursor protein was determined as described by Naqvi.[11] Test compounds were solubilized in DMSO at the desired concentration and incubated in triplicate with the enzyme for 16 hours in 96-well plates. A DMSO control (1.5 μL) and a standard inhibitor (β-secretase inhibitor IV, Calbiochem) were also tested in triplicate. The chemiluminescence signal was determined using a Fluostar Optima spectrophotometer. Data was analyzed using GraphPad Prism. BACE1 activity was calculated as a percent of the positive control using a nonlinear regression analysis function that corresponded to a best one-fit model.

Acknowledgments

This work was funded by grants to PGW from the Victoria S. and Bradley L. Geist Foundation (20070461), the Alzheimer's Association NIRG-08-90880, Alzheimer's Drug Discovery Foundation (281204), the National Institute of Aging (R20072671) and ongoing funding for biodiversity research by the Foundation for Research Science & Technology (Contract C01X0219) to the National Institute of Water & Atmospheric Research (NIWA). Funds for the upgrades of the NMR instrumentation were provided by the CRIF program of the National Science Foundation (CH E9974921) and the Elsa U. Pardee Foundation. The purchase of the Agilent LC-MS was funded by grant W911NF-04-1-0344 from the Department of Defense.

References and Notes

1. Schmitz FJ, Bloor SJ. J. Org. Chem. 1988; 53:3922–3925.
2. Cao S, Foster C, Brisson M, Lazo JS, Kingston DGI. Bioorg. Med. Chem. 2005; 13:999–1003. [PubMed: 15670907]
3. Kobayashi J, Hirase T, Shigemori H, Ishibashi M, Bae M-A, Tsuji T, Sasaki T. J. Nat. Prod. 1992; 55:994–998.
4. Roll DM, Scheuer PJ, Matsumoto GK, Clardy J. J. Am. Chem. Soc. 1983; 105:6177–6178.
5. Nakamura H, Kobayashi J, Kobayashi M, Ohizumi Y, Hirata Y. Chem. Lett. 1985; 14:713–716.
6. Alvi KA, Rodriguez J, Diaz MC, Moretti R, Wilhelm RS, Lee RH, Slate DL, Crews P. J. Org. Chem. 1993; 58:4871–4880.
7. Millán-Aguiñaga N, Soria-Mercado IE, Williams P. Tetrahedron Lett. 2010; 51:751–753.
8. Kobayashi M, Shimizu N, Kyogku Y, Kitagawa I. Chem. Pharm. Bull. 1985; 33:1305–1308.
9. Kubota T, Kon Y, Kobayashi J. Heterocycles. 2008; 76:1571–1575.
10. Ali MS, Kausar F, Malik A. J. Chem. Soc. Pak. 2001; 23:180–182.
11. Naqvi T. J. Biomol. Screen. 2004; 9:398–408. [PubMed: 15296639]

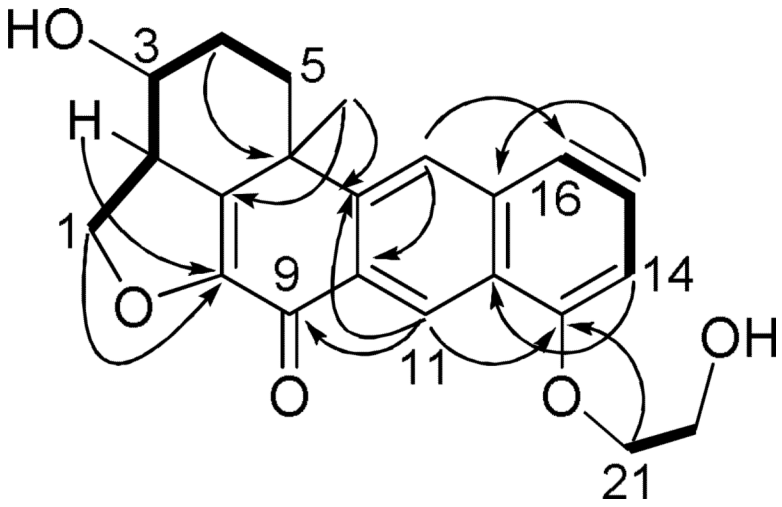

Figure 1.
Selected ^{1}H-^{1}H COSY (bold solid bars) and ^{1}H-^{13}C HMBC (arrows) Correlations Observed in the Spectra of **1**.

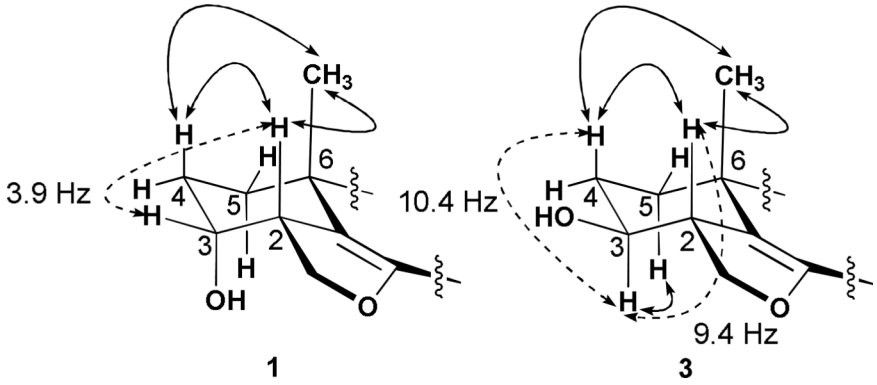

Figure 2.
Selected ROESY correlations of **1** and **3** along with key $^{3}J_{H,H}$ values (Dashed).

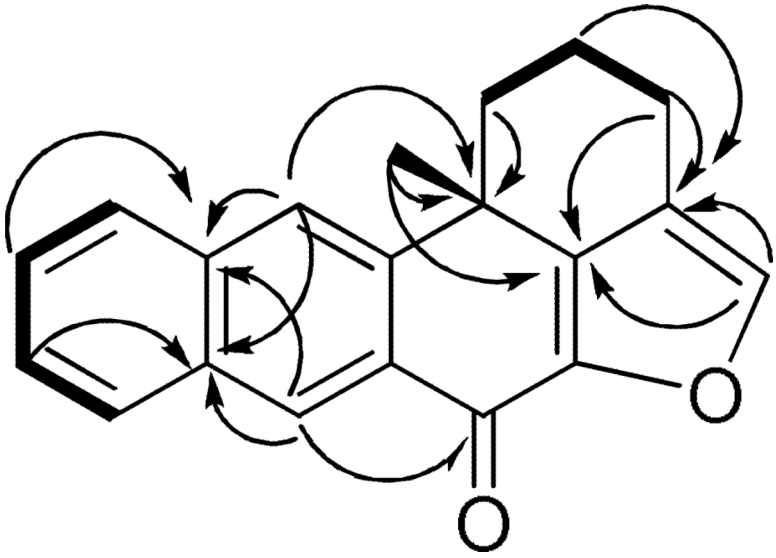

Figure 3.
Selected ^{1}H-^{1}H COSY (bold solid bars) and ^{1}H-^{13}C HMBC (arrows) correlations of **8**.

Table 1

^{1}H NMR Spectroscopic Data (500 MHz, δ_H (J in Hz)) for Compounds 1-5 (MeOH-d_4 for 1-4, $CDCl_3$ for 5).

H#	1	2	3	4	5
1	4.65, t (9.6) 4.63, dd (9.6, 7.2)	4.64, t (9.6) 4.62, dd (9.6, 7.2)	4.73, t (9.6) 4.53, dd (9.6, 6.0)	4.74, t (9.6) 4.49, dd (9.6, 6.0)	4.71, t (9.4) 4.69, dd (9.4, 7.2)
2	3.62, ddd (9.6, 7.2, 3.9)	3.62, ddd (9.6, 7.2, 4.0)	3.39, td (9.6, 6.0)	3.39, td (9.6, 6.0)	3.56, ddd (9.4, 7.2, 4.0)
3	4.06, br. dd (3.9, 3.5)	4.07, br. d (4.0)	3.51, ddd (10.4, 9.4, 4.4)	3.51, td (9.6, 4.4)	4.13, br. d (4.0)
4	1.92, tdd (14.0, 6.2, 3.5) 2.10, m	1.92, m 2.10, m	1.90, ddd (13.5, 4.4, 3.5) 1.98, dddd (13.5, 10.0, 9.6, 3.1)	1.91, m 1.99, m	2.03, m
5	1.86, td (14.0, 4.4) 2.29, dt (14.0, 3.5)	1.89, m 2.29, dt (13.0, 4.5)	1.51, td (13.1, 3.5) 2.52, dt (13.1, 3.2)	1.54, ddd (13.5, 10.0 3.5) 2.54, dt (13.5, 3.5)	1.87, td (13.0, 3.0) 2.35, dt (13.0, 4.0)
11	9.21, s	9.12, s	9.20, s	8.74, s	8.80, s
13				8.03, d (8.3)	
14	6.94, dd (6.0, 2.5)	6.83, d (7.1)	6.95, dd (7.0, 1.5)	7.55, t (8.3)	7.85, d (8.5)
15	7.51, t (6.0)	7.40, t (7.1)	7.53, t (7.0)	7.62, t (8.3)	7.42, t (8.5)
16	7.50, dd (6.0, 2.5)	7.37, d (7.1)	7.51, dd (7.0, 1.5)	7.96, d (8.3)	6.90, d (8.5)
16-OMe					4.40, s
18	8.07, s	8.02, s	8.08, s	8.16, s	8.40, s
20	1.63, s	1.63, s	1.63, s	1.67, s	1.63, s
21	4.26, t (4.5)		4.26, t (4.7)		
22	4.06, t (4.5)		4.06, t (4.7)		

Table 2

^{1}H NMR Spectroscopic Data (500 MHz, δ_H (J in Hz)) for Compounds **6**-**8** in MeOH-d_4.

H#	6	7	8
1	4.65, t (9.6) 4.63, dd (9.6, 7.2)	4.66, t (9.6) 4.64, dd (9.6, 6.0)	7.70, s
2	3.63, ddd (9.6, 7.2, 4.0)	3.63, ddd (9.6, 6.0, 4.0)	
3	4.08, br. d (4.0)	4.07, br. s	2.90, br. dd (17.0, 7.9) 2.63, br. dd (17.0, 8.9)
4	2.11, m 1.93, m	1.93, m 2.11, m	2.19, m 2.32, m
5	1.88, td (13.0, 3.5) 2.29, dt (13.0, 4.2)	1.90, m 2.32, dt (13.5, 3.5)	1.79, td (12.8, 4.2) 2.71, dt (12.8, 3.5)
11	8.65, s	8.75, s	8.80, s
13	7.50, d (8.0)	8.03, d (8.3)	8.03, d (8.3)
14	7.33, t (8.0)	7.54, t (8.3)	7.55, t (8.3)
15	6.93, d (8.0)	7.37, t (8.3)	7.63, t (8.3)
16		7.96, d (8.3)	7.95, d (8.3)
18	8.43, s	8.15, s	8.09, s
20	1.64, s	1.65, s	1.55, s

Table 3

^{13}C NMR Spectroscopic Data (125 MHz, δ_C) for Compounds **1-3**, **5-6**, **8**.

	1	**2**	**3**	**5**	**6**	**8**
C-l	72.5	72.5	75.2	71.3	72.5	146.0
C-2	48.5	48.5	51.2	47.1	48.5	122.1
C-3	68.6	68.6	76.5	67.8	68.6	19.9
C-4	29.9	29.9	31.5	28.6	29.9	18.5
C-5	35.9	35.9	39.0	34.8	36.2	30.0
C-6	39.6	39.5	39.1	38.2	39.7	38.5
C-7	142.5	142.8	142.2	143.9	142.8	149.1
C-8	148.7	148.6	148.2	147.9	148.6	145.0
C-9	178.4	178.5	178.1	176.4	178.4	173.5
C-10	130.4	129.8	130.1	132.5	131.3	142.1
C-11	123.7	124.1	123.4	127.8	128.4	130.0
C-12	125.2	125.0	125.1	137.6	134.2	132.0
C-13	157.3	156.5	157.0	121.6	121.3	130.4
C-14	106.0	109.2	106.2	126.4	128.0	127.5
C-15	130.2	130.6	130.1	105.7	111.0	129.5
C-16	120.8	119.1	120.6	154.8	154.2	128.1
C-17	137.6	137.9	137.1	130.4	127.9	135.9
C-18	126.1	125.9	126.6	119.3	120.9	124.9
C-19	149.2	149.4	149.2	145.9	147.3	147.8
C-20	26.0	26.0	25.8	25.6	26.2	34.0
C-21	71.1		71.0			

Table 4

Inhibition of BACE1

Compound	μM
1	135
2	155
3	82
4	163
5	90
6	93
7	98
8	104
	0.015